

Article

Model Study on the Combination of Operating Parameters of Corn Kernel Harvesters

Deyi Zhou, Chongbin Xu, Yuelin Xin, Pengfei Hou , Baoguang Wu *, Haiye Yu, Jinsong Zhang 
and Qiang Zhang

The College of Biological and Agricultural Engineering, Jilin University, 5988 Renmin Street, Changchun 130025, China; zhoudy@jlu.edu.cn (D.Z.); 18345978756@163.com (C.X.); meijingaifan@163.com (Y.X.); houpf20@mails.jlu.edu.cn (P.H.); haiye@jlu.edu.cn (H.Y.); jluzjs@jlu.edu.cn (J.Z.); zhangqiang@jlu.edu.cn (Q.Z.)

* Correspondence: wubg@jlu.edu.cn

Abstract: This study analyzed the engine operating condition curve of the corn kernel harvester. Field experiments identified the feed rate, concave clearance, and cylinder speed as the main factors affecting operating quality and efficiency. A ternary quadratic regression orthogonal center-of-rotation combined optimization test method was used to determine the feed rate, cylinder speed, and concave clearance as the influencing factors, and the engine speed variation rate, crushing rate, impurity rate, loss rate, and cylinder speed variation rate as the objective functions. A mathematical regression model was developed for the combination of operating quality indicators, efficiency indicators, and operating parameters of the corn kernel harvester. A non-linear optimization method was used to optimize the parameters of each influencing factor. The results showed that with a feed rate of 12 kg/s, a forward speed of 5 km/h, a cylinder speed of 360 r/min, and a concave clearance of 30 mm, the average crushing rate was 3.91%, the average impurity rate was 1.71%, and the kernel loss rate was 3.1%. This model could be used for the design and development of intelligent control systems.

Keywords: corn kernel harvesters; parameter combination model; operating quality; operating efficiency



Citation: Zhou, D.; Xu, C.; Xin, Y.; Hou, P.; Wu, B.; Yu, H.; Zhang, J.; Zhang, Q. Model Study on the Combination of Operating Parameters of Corn Kernel Harvesters. *Appl. Sci.* **2021**, *11*, 10328. <https://doi.org/10.3390/app112110328>

Academic Editors: Manuel Armada and José Miguel Molina Martínez

Received: 18 August 2021
Accepted: 1 November 2021
Published: 3 November 2021

Publisher's Note: MDPI stays neutral with regard to jurisdictional claims in published maps and institutional affiliations.



Copyright: © 2021 by the authors. Licensee MDPI, Basel, Switzerland. This article is an open access article distributed under the terms and conditions of the Creative Commons Attribution (CC BY) license (<https://creativecommons.org/licenses/by/4.0/>).

1. Introduction

Corn is the most widely distributed food crop in the world, which is grown in large quantities from latitude 53° N to 40° S [1–3]. Corn can be used not only as a kind of grain but also for feed processing, oil production, bio-energy, and other industrial fields. It is an agricultural crop with significant economic value and broad cultivation prospects [4–6].

The corn planting area is increasing year by year, and the demand for corn kernel harvesters is also growing, while the harvesters are required to have better operating quality and operating efficiency [7–10]. The leading indicators for evaluating the operating quality of crop harvesters are the impurity rate, the crushing rate, and the crop kernel loss rate; one of the indicators for assessing the operational efficiency of crop harvesters is the blockage failure rate [11–14]. These evaluation indicators also could be applied to corn kernel harvesters.

Improving the operating quality and efficiency of harvesters could reduce the loss of corn kernels and profit loss caused by harvesters. Therefore, some studies have been carried out to improve the operating quality and efficiency of harvesters [15–18]. Wan et al. used computer vision technology to recognize the shape of corn kernels and constructed a BP neural network with grain shape feature parameters to detect the grain shape of corn kernels and determine the rate of broken kernels [19]. Mahirah et al. designed a machine vision system with dual front and rear light illumination to detect the impurity rate and corn kernel crushing rate through image acquisition and image analysis algorithms [20]. Chen et al. obtained the raw spectra of wheat samples and established a spectral inversion model of wheat impurity by component analysis, which could quickly detect the impurity

of wheat [21]. Currently, methods to reduce the failure rate are mainly based on monitoring and alarming. The harvester operating environment is harsh and the sensor detection data are prone to distortion, which may not prevent the appearance of harvester failures, such as cylinder clogging [22]. The methods used to improve the operational quality and operational efficiency of corn kernel harvesters are manual post-hoc regulation of the harvester parameters and relying on operator experience, which is less efficient and cannot be universally applied to most harvesting operating environments, and also does not allow the harvester to work with a better combination of operating parameters [23,24].

This study analyzed the influence of several combined factors on the operating quality and efficiency, which were closely related to the engine speed, power, and load of the corn kernel harvester. The relationship curves of the engine speed and feeding capacity of the corn kernel harvester, the threshing cylinder speed and the feeding capacity, and the engine speed and the threshing cylinder speed were obtained through field tests. Through data processing and analysis using Data Processing System (DPS) V9.0.1, a regression model of the operating quality index, the efficiency index and the operating parameter combination of a corn kernel harvester was obtained. This model could obtain the optimized combination of operating parameters, so that the harvester could work under the optimized combination of operating parameters to achieve better operating quality and efficiency.

This study provides a new solution to improve the operating quality and operating efficiency of harvesters. The operation parameter combination model could be used for the design and development of intelligent control systems for harvesters. The purpose of the study is to examine the relationships of the feed rate, concave clearance, and cylinder speed with the operating quality and operating efficiency of the harvester. In the meanwhile, the focused target of this study was to investigate the coupling effect of multiple factors in the same group of experiments.

2. Analysis of the Principles

The threshing cylinder is an essential working part of corn kernel harvesters. The feed rate, the concave clearance, and the speed of the threshing cylinder directly affect the operating quality and efficiency of the harvester. The engine provides power for the threshing cylinder; the speed of the threshing cylinder and all the moving parts of the harvester is determined by the engine speed. The harvester can work normally only when the engine speed is within a certain range. If the engine speed fluctuates drastically, it will lead to poor operating quality and even failures such as threshing cylinder blockage.

2.1. Working Principle of a Harvesting Machine Threshing Cylinder

The corn cob is fed through the inlet. In the threshing chamber, it is hit and rubbed by the high-speed rotating threshing cylinder. The corn kernels fall off, and the kernels are separated by a sieve to achieve threshing. According to the analysis of Equation (1), when the threshing cylinder rotates steadily at a constant speed, the power N transferred from the engine to the threshing cylinder is equal to the power loss caused by the threshing cylinder overcoming the frictional force of the motion, air resistance, and threshing resistance. When the feeding quantity q increases, the concave clearance decreases (that is, the rubbing coefficient f increases), the threshing resistance power increases, the speed of the disengaging cylinder increases (i.e., that is the angular speed ω increases), and the power transferred from the engine to the threshing cylinder is required to increase [25]. The symbols of Equation (1) are shown in Table 1.

$$J\omega \frac{d\omega}{dt} = N - (a\omega + b\omega^3) - \frac{qr^2}{2(1-f)} \frac{\gamma + \lambda}{1 + \lambda} \quad (1)$$

Table 1. Equation symbol table.

Symbols	Meaning	Symbols	Meaning
ω	Angular velocity (rad/s)	r	Equivalent radius (m)
$\frac{d\omega}{dt}$	Angular acceleration (rad/s ²)	J	Rotational inertia (kg·m ²)
W_e	Circulation function	N	Power (kW)
γ	Crop grain to grass ratio	q	Feed rate (kg/s)
f	Rubbing factor	a	Coefficients of friction
λ	Ratio of stalk exit velocity to the circumferential velocity of threshing cylinder	b	Air resistance

2.2. Harvester Engine Working Condition Analysis

When the harvester is in operation, the speed of the various working parts, such as the header, threshing cylinder, and cleaning screen, has a fixed relationship with the drive system and engine speed. The harvester can work normally only when the engine speed is within a certain range. Figure 1 shows a diagram of the harvester engine operating conditions, with the shaded area showing the normal operating area of the harvester. In the AB region, before the maximum output torque $T_{tq,max}$ is reached, the output power P_e and the output torque increase with increases in the load. In the BC region, after the output torque reaches the maximum output torque $T_{tq,max}$, the output power P_e continues to increase and the output torque decreases as the load increases. In the CD region, after the output power reaches the maximum output power $P_{e,max}$, with the load increasing, the output torque T_{tq} and the output power P_e decrease sharply. At this point, the engine speed is reduced to a certain value by the increasing load; meanwhile, the harvester’s operating quality is reduced, which could even lead to faults such as clogging of the threshing cylinder [26].

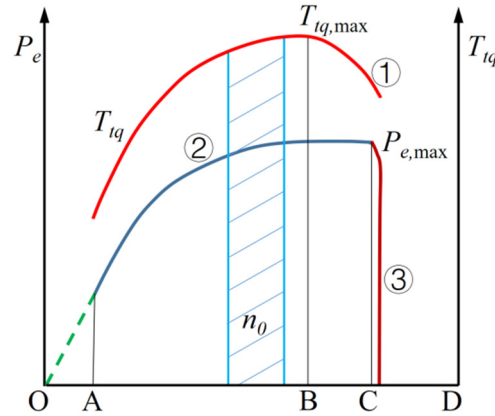


Figure 1. Harvester engine operating conditions diagram: P_e —engine output power; n —engine speed; T_{tq} —output torque; $T_{tq,max}$ —maximum output torque; $P_{e,max}$ —maximum output power; ①—output torque curve; ②—output power curve during normal operation; ③—overload power curve.

The increase in the feed rate, the reduction in the concave clearance, and the increase in the speed of the threshing cylinder will all cause an increase in the harvester’s engine load and require an increase in the engine’s output power. When the output power reaches the maximum output power, the load of the harvester engine increases, which causes the harvester engine speed and output power to decrease. When the harvester’s engine speed decreases above a certain value, the harvester cannot operate normally, its operating efficiency reduces, and it will be prone to blockages and other failures.

3. Materials and Methods

3.1. Experimental Method

3.1.1. Experimental Field

The field trial was conducted in mid-October 2020 at the agricultural experimental base of Jilin University. The corn variety was Xianyu 335. The average plant height was 310 cm. The average plant spacing was 28 cm and the average moisture content of the corn kernels at harvest was 27%. The model of moisture meter was MA50/1.R, which has an accuracy of 1×10^{-6} .

As shown in Figure 2, the harvester used for the field experiment was a modified John Deere 1075 harvester, based on the original frame. The harvester was converted to a corn kernel harvester with a single longitudinal axial threshing system. The harvester control system was a Wecon LX3V-1412MR PLC, which was made in China. Magneto-electric speed sensors were installed at the threshing cylinder and engine shaft end to detect the harvester's speed and the threshing cylinder's speed.



Figure 2. Harvester speed detection: (a) detection of the re-detachment speed; (b) upper kernel speed; (c) speed indicator; (d) detection of cylinder speed.

The corn harvester operated on 6 rows, with an effective cutting width of 3280 mm, a cylinder speed of 300 to 900 r/min, a concave clearance of 20 to 40 mm, and an operating speed of 2 to 8 km/h. In this experiment, the corn row distance was 600 mm.

3.1.2. Corn Yield Determination

To measure the yield per unit of area of corn, the feed rate q could be calculated. Three side-by-side strip test plots were selected in the field, and three square sampling areas with a side length of 2 m were evenly selected in each strip test plot. To prevent uneven growth of corn at the head of the field due to environmental influences affecting the cob harvest, a distance of 20 m from the head of the field on both sides of the test field was excluded before sampling, as shown in Figure 3. The average crop mass per unit of area, m , of the 9 sets of data collected was used as the crop density for this experiment. The unit area crop mass record sheet is shown in Table 2.

The crop feed rate at different stalls could be calculated according to Equation (2):

$$q = d \cdot v \cdot m \quad (2)$$

In Equation (2): q is the feed rate (kg/s), d is the effective cutting width of the harvester (m), v is the forward speed (m/s), and m is the crop mass per unit of area.

The distance between each single furrow was 600 mm in this experiment, which is shown in Figure 4.

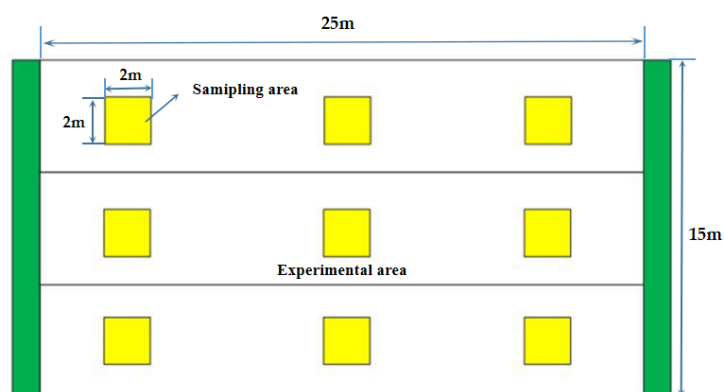


Figure 3. Diagram of the trial field.

Table 2. Unit area crop quality record sheet.

No.	Crop Mass Per Unit of Area (kg/m ²)		
Region 1	2.58	2.67	3.09
Region 2	2.58	3.22	2.01
Region 3	2.36	2.81	2.86
Average crop mass per unit area	2.69		

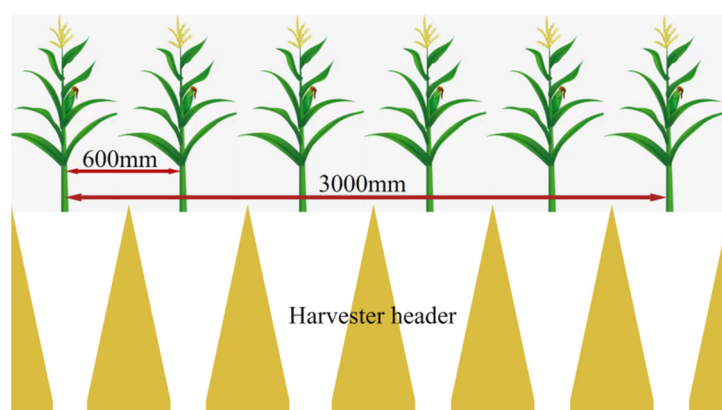


Figure 4. Harvester header field operation status diagram.

3.2. Indicators of Experiment Factors and Operational Parameters

This experiment used a ternary quadratic regression orthogonal center of rotation combination test method, which was able to conduct the effect of the multi-test factors on the multi-response factors in this test [27].

In the field experiments, the concave clearance could not be adjusted in real time, so the concave clearance was set to 20 mm, 25 mm, 30 mm, 35 mm, and 40 mm before the operation, depending on the actual operation.

During operation, five speeds in the range of 3–7 km/h evenly distributed in the forward speed range were selected. The feed rate was taken to be in the range of 7.35–17.15 kg/s.

The cylinder speed was taken as 300 to 420 r/min. The initial engine speed was set at 2200 r/min and the initial cylinder speed was 360 r/min, accelerating or decelerating once for a 40 m advance. The speed varied from 3 km/h to 7 km/h to 3 km/h. The change in engine speed and cylinder speed on the monitor was recorded. The experimental factors were coded as shown in Table 3.

Table 3. Experimental factors and codes.

Code	Factors		
	Feed Rate: q (kg/s)	Cylinder Speed: n (r/min)	Concave Clearance (mm)
1.6818	17.15	420	40
1	14.70	390	35
0	12.25	360	30
−1	9.8	330	25
−1.6818	7.35	300	20

For each test, a 2000 g test sample was picked up from the kernel tank interface. Impurities were selected from the sample and weighed, and the impurity rate was calculated according to the formula. Corn kernels with machine damage and visible cracks were selected from the sample and weighed, and the broken kernel mass was calculated according to the formula to obtain the crushing rate. In each group of operating areas, three areas of 4 m² were selected. All kernels lost on the ground were picked up in the sampling area, including broken corn ears less than 5 cm in length. The mass was weighed after shedding. The loss rate was calculated according to Equation (5).

The crushing rate, loss of kernels to the ground, and the rate of trashing are the main indicators used to evaluate the operating quality of a harvester.

The formula is calculated as:

$$Z_S = \frac{W_s}{W_i} \times 100\%, \quad (3)$$

In Equation (3), W_s is the total mass of crushed seeds, in g; W_i is the total mass of sample seed, in g; and Z_S is the corn kernel crushing rate, in %.

$$Z_z = \frac{W_{za}}{W_h} \times 100\%, \quad (4)$$

In Equation (4), W_h is the mixed kernel mass in g; W_{za} is the impurity mass, in g; and Z_z is the impurity rate, in %;

$$S_L = \frac{W_L}{W_Z} \times 100\%, \quad (5)$$

In Equation (5), W_Z is the total mass of kernels, in g; W_L is the total mass of corn lost, in g; and S_L is the corn kernel loss rate, in %.

$$\delta = \frac{n_1 - n_0}{n_0} \times 100\%, \quad (6)$$

In Equation (6), δ is the engine speed variation rate, in %; n_1 is the engine speed at the rated load, in r/min; and n_2 is the engine speed without load, in r/min.

$$\Delta n = \frac{n_{\max} - n_{\min}}{n_{\min}} \times 100\%. \quad (7)$$

In Equation (7), Δn is the engine speed variation rate, in %; n_{\max} is the maximum speed of the disengaging cylinder at the rated load, in r/min; and n_{\min} is the threshing cylinder speed without a load, in r/min.

3.3. Experimental Scheme Design Based on Ternary Quadratic Regression of the Orthogonal Center-of-Rotation Combination Optimization Test

In this experiment, the feed rate q , the cylinder speed n , and the concave clearance were used as experimental factors; x_1 , x_2 and x_3 indicate the coded values. Engine speed variation rate, crushing rate, concave clearance, corn kernel loss rate, and cylinder speed variation rate were taken as the response values for the engine speed variation rate; y_1 , y_2 , y_3 , y_4 and y_5 indicate the coded values.

The software DPS V9.0.1 was used for data processing and analysis. A table of ternary secondary generic combination design parameters was automatically generated using the DPS software data processing system. The significance of each factor's effect on the regression model was tested by the *F*-test, and a non-linear optimization calculation method was used to obtain the optimal combination of parameters that met the requirements.

4. Results and Discussion

4.1. Experimental Results of a Ternary Quadratic Regression of the Orthogonal Center of Rotation Combination Optimisation Test

In this experiment, the feed rate q , the cylinder speed n , and the concave clearance were taken as experimental factors; x_1 , x_2 , and x_3 were denoted their coded values, respectively. The engine speed variation rate, crushing rate, corn kernel loss rate, and cylinder speed variation rate were taken as response values; y_1 , y_2 , y_3 , y_4 , y_5 represent the code values. The test results are shown in Table 4. A change rate of 100% was the shutdown state in Table 4.

Table 4. Experimental scheme and results.

Levels	Feed Rate	Cylinder Speed	Concave Clearance	Engine Speed Variation Rate	Crushing Rate	Impurity Rate	Kernel Loss Rate	Cylinder Speed Variation Rate
	x_1	x_2	x_3	y_1	y_2	y_3	y_4	y_5
1	1	1	1	100	3.33	1.96	9.10	100
2	1	1	-1	100	2.72	0.94	2.33	100
3	1	-1	1	0.14	4.84	1.24	4.19	7.62
4	1	-1	-1	1.42	4.57	1.66	3.07	3.61
5	-1	1	1	2.60	4.97	2.58	8.71	4.10
6	-1	1	-1	6.85	2.93	1.89	3.44	9.17
7	-1	-1	1	100	3.80	1.31	19.85	100
8	-1	-1	-1	3.47	4.45	1.61	6.95	4.33
9	-1.6818	0	0	0.29	3.76	2.58	22.15	4.72
10	1.6818	0	0	2.31	7.45	1.34	16.67	4.10
11	0	-1.6818	0	1.48	4.18	0.86	5.63	2.42
12	0	1.6818	0	12.23	4.83	0.89	4.99	15.56
13	0	0	-1.6818	23.66	4.16	0.77	3.35	22.78
14	0	0	1.6818	12.67	5.71	1.48	4.41	14.44
15	0	0	0	0.65	3.56	2.90	38.19	1.11
16	0	0	0	1.60	3.57	0.95	3.53	3.03
17	0	0	0	0.42	4.17	2.00	4.28	1.11
18	0	0	0	0.46	4.24	1.10	2.47	1.54
19	0	0	0	0.05	4.23	2.60	3.15	0.28
20	0	0	0	11.86	5.07	1.75	8.61	13.33

4.2. Harvester Engine Speed in Relation to Threshing Cylinder Operating Parameters

As shown in Figure 5a, there was a linear relationship between threshing cylinder speed and the engine speed, and the root mean square error of the linear fit was 0.8819. When the harvester was operating in the field, the engine operated at a constant speed, so the threshing cylinder speed was constant, which ensured the operating quality. Reducing fluctuations in the engine speed meant reducing fluctuations in the threshing cylinder speed, which would have reduced fluctuations in the operating quality of the harvester.

Figure 5b shows that the engine load increased with an increase in the forward speed and feed rate. At a concave clearance of 20 mm, when the output power reached the maximum output power $P_{e,max}$, the engine speed started to drop continuously from 2200 r/min; the cylinder speed dropped simultaneously. When the engine speed dropped around 1800 r/min, the cylinder was observed to have a tendency to clog. After dropping to 1700 r/min, the cylinder clogged, which subsequently reduced the feed rate. The engine load decreased, then the engine speed and cylinder speed rose back to the set value. The threshing cylinder speed and engine speed increased or decreased with the curve of the change in feed rate. With a concave clearance of 30 mm or 40 mm, when the output

power reached the maximum output power $P_{e,max}$, the engine speed began to decline continuously from 2200 r/min, but the engine speed variation rate was less than 10%. The trend of change was close to that at 20 mm concave clearance, and it could still operate at a higher feed rate.

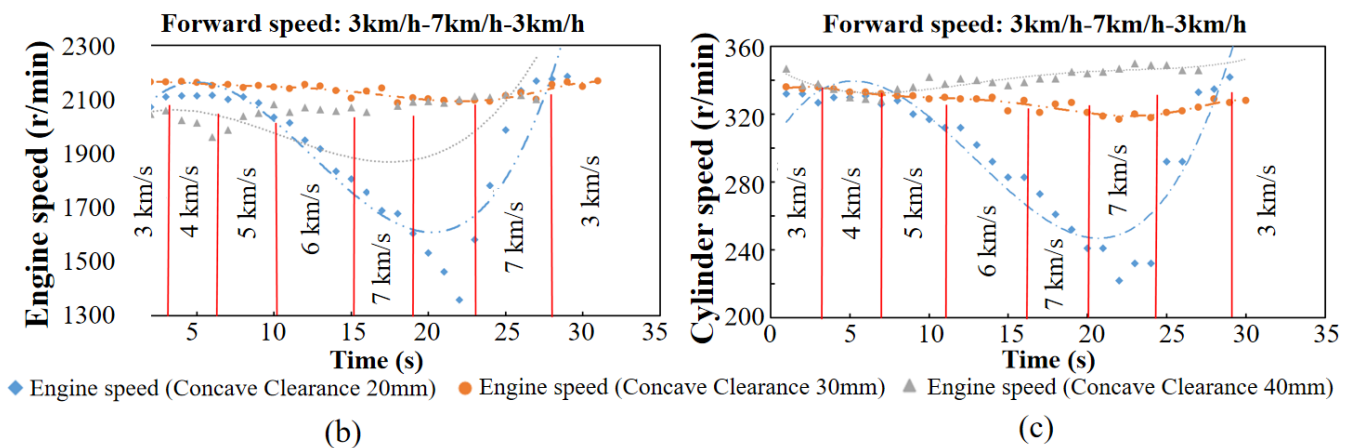
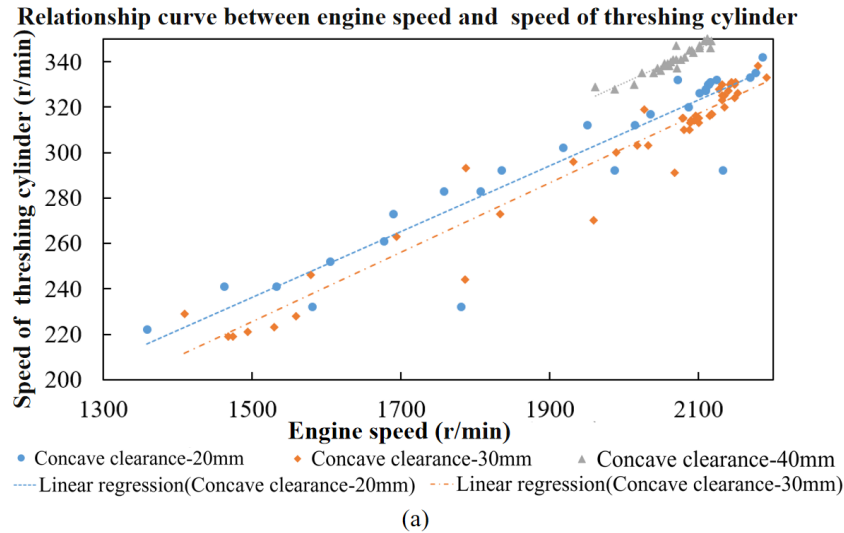


Figure 5. The relationship curve between engine speed and feed rate, cylinder speed, and concave clearance. (a) The relationship curve between the engine speed and threshing cylinder speed of the harvester. (b) Curve of engine speed change with the feed rate. (c) Curve of cylinder speed change with the feed rate.

Figure 5b,c shows that the engine speed of the test group with a 20 mm concave clearance fluctuated the most sharply when the feed rate increased. The fluctuation in the engine speed would lead to a decrease in harvest quality. This indicates that the concave clearance of 20 mm had a greater influence on the engine speed. The concave clearance could be chosen to be different from 20 mm; 30 mm to 40 mm could be selected. Meanwhile, the operating efficiency could be improved by increasing the feed rate. However, at different concave clearances, changes in the feed rate would cause changes in the engine speed n and the output power P_e . Thus, to ensure operating quality, a suitable feed rate should be selected.

In Figure 5, as the concave clearance increased, the fluctuation in engine and cylinder speed slowed down, even if the feed rate increased. The harvester’s operating quality was improved by adjusting the feed rate, the concave clearance, and threshing cylinder speed; the concave clearance was not easy to adjust in real time and a concave clearance value was pre-selected before the operation, followed by adjustment of the threshing cylinder speed and finally the feed rate. When the engine speed was reduced by more than 10%, there was a tendency towards blockage and adjustment was required; when the harvester engine

speed was reduced by 20%, both its speed n and output power P_e dropped rapidly and serious blockage occurred in the harvester. When the engine speed fell below the minimum engine speed, the engine stalled and the harvester stopped. Therefore, the experiment's conclusions were consistent with the analysis of the principles and provided guidance for selection of the harvester's operating parameter combinations.

4.3. Optimization of Operating Parameters

4.3.1. Operating Quality Contour Plots

Figure 6 shows contour maps of the crushing rate, impurity rate, loss rate, the engine speed variation rate, and the cylinder speed variation rate. According to the target operating quality indicators, a suitable combination of operating parameters could be found on the contour plot. In Figure 6, the crushing rate, impurity rate, corn kernel loss rate, the engine speed variation rate, and the cylinder speed variation rate could be kept in a low range when operating with a cylinder speed of 350 to 370 r/min, a forward speed of 4 to 6 km/h, and a concave clearance of 27 to 35 mm.

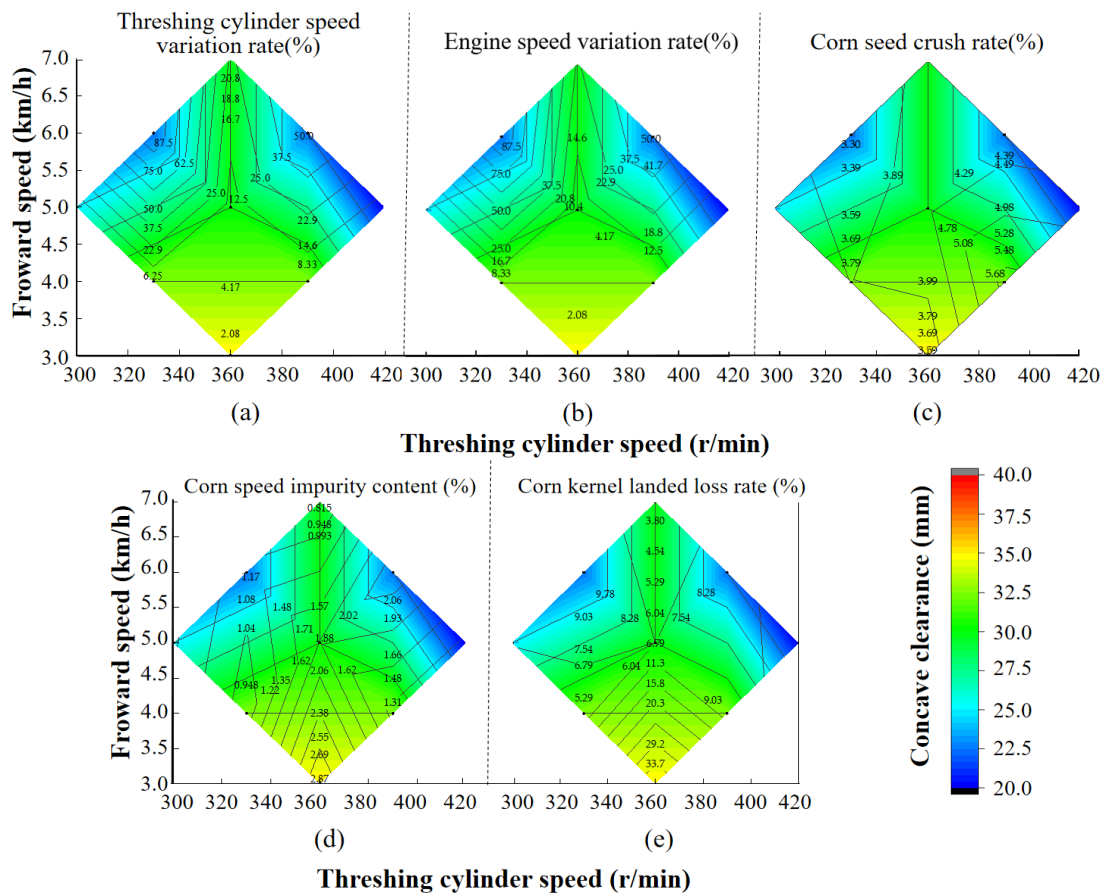


Figure 6. Contour maps of operating quality. (a) Threshing cylinder speed variation rate; (b) engine speed variation rate; (c) corn kernel crushing rate; (d) corn kernel impurity rate; (e) corn kernel loss rate.

4.3.2. Regression Analysis

The DPS software was used to process the test data. The regression coefficients in the regression equation were tested by the F -test at a significance level of 0.05, taking the engine speed variation rate y_1 , the crushing rate y_2 , the impurity rate y_3 , the corn kernel loss rate y_4 , and the cylinder speed variation rate y_5 as the objective functions. The regression equation was as follows:

$$y_1 = 1.53 + 6.74x_1 + 8.97x_2 + 5.31x_3 + 5.94x_1^2 + 7.90x_2^2 + 11.90x_3^2 + 36.56x_1x_2 - 11.69x_1x_3 - 12.44x_2x_3, \tag{8}$$

$$y_2 = 4.18 + 0.40x_1 - 0.19x_2 + 0.38x_3 + 0.28x_1^2 - 0.11x_2^2 + 0.05x_3^2 - 0.38x_1x_2 - 0.06x_1x_3 + 0.38x_2x_3, \tag{9}$$

$$y_3 = 1.87 - 0.27x_1 + 0.12x_2 + 0.16x_3 + 0.10x_1^2 - 0.28x_2^2 - 0.19x_3^2 - 0.19x_1x_2 + 0.03x_1x_3 + 0.30x_2x_3, \tag{10}$$

$$y_4 = 10.11 - 2.16x_1 - 0.85x_2 + 2.04x_3 + 2.83x_1^2 - 2.16x_2^2 - 2.67x_3^2 + 2.35x_1x_2 - 1.29x_1x_3 - 0.24x_2x_3, \tag{11}$$

$$y_5 = 1.91 + 0.29x_1 - 0.34x_2 + 3.42x_3 + 1.56x_1^2 + 2.23x_2^2 + 2.83x_3^2 + 6.93x_1x_2 - 3.71x_1x_3 - 3.37x_2x_3. \tag{12}$$

A mathematical regression model was obtained from the analysis of variance (ANOVA); the ANOVA results are shown in Table 5. As can be seen in Table 5, the significance test of $y_2, y_3,$ and y_4 was $F_2 > 3.02, 1 > p > 0.05,$ which was less significant but had a tendency to be significant. The main reason for this was that the factors affecting the crushing rate, impurity rate, and loss rate were not limited to the three mentioned in the text. For example, the parameters of wind speed and scavenging section would determine the size of the impurity rate to some extent. The y_1 parameter had a good fit, with a significance test of $F_2 = 3.519, p = 0.0359 < 0.05,$ indicating that the regression equation was significant. The y_5 parameter also had a good fit, with a significance test of $F_2 = 3.473, p = 0.0373 < 0.05,$ indicating that the regression equation was significant.

Table 5. Analysis of variance.

	Source	Sum of Squares	Degrees of Freedom	Mean Square	F-Value	p-Value
y_1	Regression	18,078.18	9	2008.69	$F_2 = 3.519$	0.036
	Remainder	5708.35	10	570.84	—	—
	Lack of fit	5602.13	5	1120.43	$F_1 = 52.74$	0.0001
	Pure error	106.23	5	21.25	—	—
	Total	23,786.53	19	—	—	—
y_2	Regression	8.22	9	0.91	$F_2 = 0.74$	0.6812
	Remainder	12.40	10	1.24	—	—
	Lack of fit	10.86	5	2.17	$F_1 = 7.00$	0.0047
	Pure error	1.55	5	0.31	—	—
	Total	20.62	19	—	—	—
y_3	Regression	4.40	9	0.35	$F_2 = 1.309$	0.35
	Remainder	3.74	10	—	—	—
	Lack of fit	—	5	—	$F_1 = 0.219$	0.95
	Pure error	—	5	—	—	—
	Total	—	19	—	—	—
y_4	Regression	498.31	9	55.37	$F_2 = 0.528$	0.83
	Remainder	1049.31	10	104.93	—	—
	Lack of fit	74.40	5	14.88	$F_1 = 0.076$	0.99
	Pure error	974.91	5	194.98	—	—
	Total	1547.62	19	—	—	—
y_5	Regression	17,318	9	1924.22	$F_2 = 3.473$	0.0373
	Remainder	5539.78	10	553.978	—	—
	Lack of fit	5417.28	5	1083.46	$F_1 = 44.223$	0.0001
	Pure error	122.499	5	24.4999	—	—
	Total	22,857.8	19	—	—	—

4.3.3. Operating Parameter Optimization

MATLAB was used to optimize and calculate the regression equation. Combined with the actual operating parameter indicators, the crushing rate was less than 5%, the impurity rate was less than 2%, the kernel loss was less than 5%, and the critical indicators for engine speed and cylinder speed were 10% and 20% respectively. That is, if the speed variation rate exceeded 10%, there would be a tendency toward blockage, and processing adjustment

would be required; if the speed variation rate exceeded 20%, the harvester experienced severe blockage. The range of the individual operating parameters was obtained after the optimization calculations.

To analyze the relationships among the influencing factors, including the feed rate, concave clearance, and cylinder speed, and the target functions (crushing rate, impurity rate, and corn kernel loss rate), and to optimize the combination of operating parameters, scatter plots and the box plots of the feed rate, concave clearance and cylinder speed were obtained with the aid of Origin software.

In the box diagram, the horizontal lines above and below the boxes are the 25% quantile position and the 75% quantile position of the sample, respectively; the boxes contain 50% of the data in the sample.

Figure 7 shows the scatter plots and box plots of the values of the feed rate x_1 obtained by optimizing the regression model with the actual operating indicators. In Figure 7a, it can be seen that the range of values of the solution for the feed rate x_1 calculated by the regression model optimization was concentrated between 12 kg/s and 13 kg/s. In Figure 7b, it can be seen that the optimal feed rate range after the optimized calculation of the rate of change of engine speed y_1 and cylinder speed y_5 was mainly distributed around 12 kg/s; that is, the forward speed of the harvester was about 5 km/h. From the scatter distribution outside the box line, the lower the system feed rate, the lower the system speed variation, which suggested that the system's operation was more stable. The influence of the feed rate x_1 on the impurity rate y_3 was relatively large, with the feed rate x_1 obtained at an impurity rate of 2% being concentrated below 12 kg/s. The optimum operating speed of the harvester could be selected between 3 and 5 km/h, provided that the impurity rate met the target operating quality index.

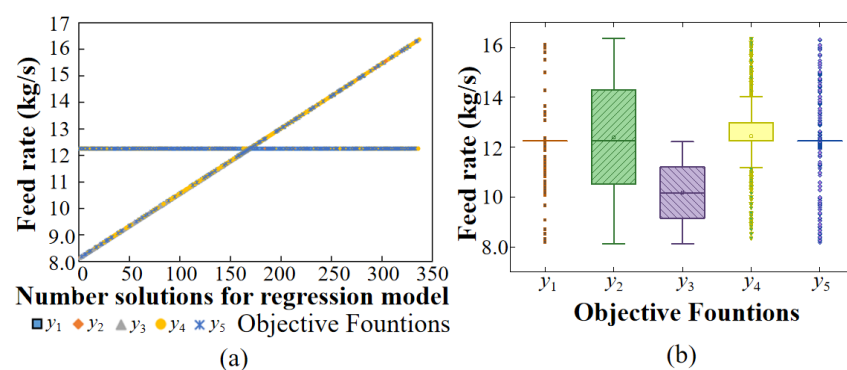


Figure 7. Feed rate: (a) Scatter plot of feed rate. (b) Box graph of feed rate: y_1 —engine speed variation rate; y_2 —crushing rate; y_3 —impurity rate; y_4 —corn kernel loss rate; y_5 —cylinder speed variation rate.

Figure 8 shows the scatter plot and box plot of the cylinder speed x_2 values obtained after the regression model was optimized in conjunction with the actual operating indicators. As shown in Figure 8, the optimized cylinder speed x_2 was calculated to be above 360 r/min. In Figure 8a, the values of the engine speed variation rate y_1 and the cylinder speed variation rate y_5 were mostly concentrated around 360 r/min; the engine worked more smoothly at 360 r/min, and the corn kernels loss rate on the ground was also lower at this rotational speed. It was possible to select 360 r/min as the initial parameter during operation, but it was also possible to adjust it according to the actual situation and make the crushing rate y_2 and other indicators lower by adjusting the speed appropriately.

Figure 9 shows the scatter plot and box diagram of the distribution of the concave clearance values x_3 solved by the model. In the box diagram, it can be seen that the engine speed variation rate y_1 and the cylinder speed variation rate y_5 were at the optimum value when the concave clearance was around 30 mm. The impurity rate was the least sensitive to the concave clearance x_3 and the distribution of the solutions was very wide; the crushing rate y_2 was the lowest when the concave clearance x_3 was around 35 mm. In the scatter plot, it can be seen that the solutions of other models were distributed around 30 mm,

where the data were the most densely distributed. Therefore, the optimum operating parameters were a feed rate x_1 of 12 kg/s, a cylinder speed x_2 of 360 r/min, and a concave clearance of 30 mm.

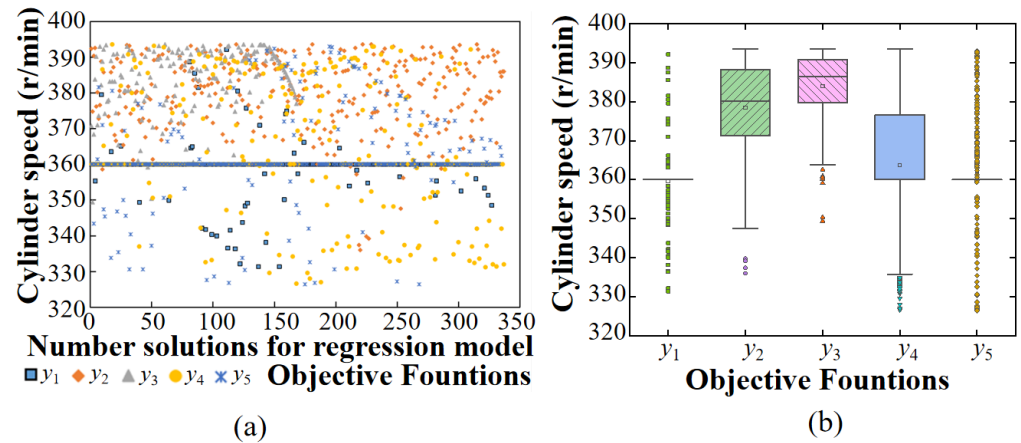


Figure 8. Cylinder speed: (a) Scatter plot of cylinder speed. (b) Box diagram of cylinder speed: y_1 —engine speed variation rate; y_2 —crushing rate; y_3 —impurity rate; y_4 —corn kernel loss rate; y_5 —cylinder speed variation rate.

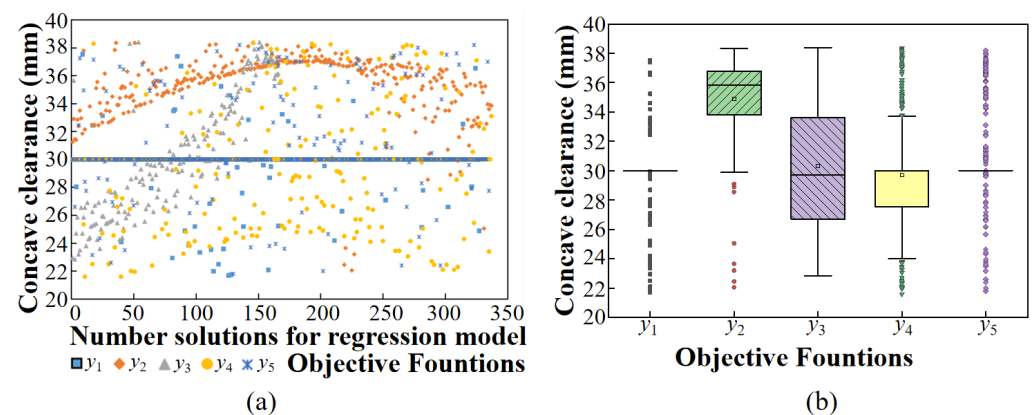


Figure 9. Box diagram of the distribution of concave clearance values. (a) Scatter plot of concave clearance. (b) Concave clearance box line diagram: y_1 —engine speed variation rate; y_2 —crushing rate; y_3 —impurity rate; y_4 —corn kernel loss rate; y_5 —cylinder speed variation rate.

Therefore, the optimal operating parameters were a feed rate of 12 kg/s, a cylinder speed of 360 r/min, and a concave clearance of 30 mm. In a comparison of the contour plots in Figure 5, it was found that the optimal operating parameters range were a feed rate x_1 of 9.8 to 12.25 kg/s, a forward speed of 4 to 5 km/h, a cylinder speed x_2 of 330 to 370 r/min, and a concave clearance x_3 of 30 mm, while satisfying the engine speed variation rate y_1 of less than 5%, a cylinder speed variation rate y_5 of less than 10%, a crushing rate y_2 of less than 5%, an impurity rate y_3 of less than 2%, and a corn kernel loss rate y_4 of less than 4%.

4.4. Experimental Validation of Operating Parameters

The optimum combination of parameters was verified by using the same test conditions as in the previous test, using the modified John Deere 1075 harvester in the field operation. The combinations of operating parameters were divided into two groups to continue the test; Group 1: feed rate = 9.8 kg/s, cylinder speed = 360 r/min, concave clearance = 30 mm; Group 2: feed rate = 12.25 kg/s, cylinder speed = 360 r/min, concave clearance = 30 mm. Each group of experiments was repeated three times, as shown in Table 5. As shown in Figure 8, Group 2 (feed rate = 12.25 kg/s, cylinder speed = 360 r/min, concave clearance = 30 mm) had a lower impurity rate, a lower crushing rate, and a lower corn kernel loss rate than

Group 1 (feed rate = 9.8 kg/s, cylinder speed = 360 r/min, concave clearance = 30 mm), so Group 2 was chosen as the better choice. The harvester worked better with the parameter combination of Group 2. These were lower than the Chinese national standards, with a crushing rate of less than 5%, an impurity rate of less than 3%, and a loss rate of less than 5%. The correctness of the regression model was verified as shown in Figure 10.

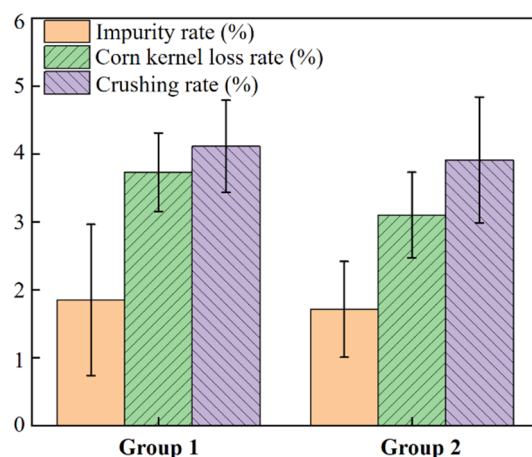


Figure 10. Parametric verification quality data statistics graph.

5. Conclusions

This study analyzed the engine operating conditions curve of a corn kernel harvester during operation. The relationship curves of the engine speed and feed rate, the threshing cylinder speed and feed rate, and the engine speed and threshing cylinder speed were obtained from field trials.

The ternary quadratic regression of the orthogonal center-of-rotation combination optimization test method was used to produce an operating quality contour plot, from which a better combination of operating parameters could be found. A mathematical regression model was fitted using DPS V9.0.1 software to relate the influencing factors to the operating efficiency and operating quality. The effects of the feed rate, cylinder speed, and concave clearance on the corn kernel loss rate, impurity rate, engine speed variation rate, and cylinder speed variation rate were investigated.

By setting the boundary conditions for the target quality indicators (a crushing rate less than 5%, an impurity rate less than 2%, a corn kernel loss rate less than 5%, and the threshold value for the engine speed and cylinder speed variation rate of 10%), a better combination of operating parameters was obtained by this model, which was a feed rate of 12 kg/s, a forward speed of 5 km/h, a threshing cylinder speed of 360 r/min, and a concave clearance of 30 mm, which was consistent with the combination of operating parameters obtained from the contour plot of the operating quality indicators. The harvester was tested in the field with this combination of operating parameters and obtained a good operating quality, with an average crushing rate of 3.91%, an average impurity rate of 1.71%, and an average corn kernel loss rate of 3.1%. The harvester operating with the combination of parameters derived from this model was able to achieve excellent operating quality and operational efficiency.

Author Contributions: Conceptualization, D.Z. and B.W.; validation, C.X., Y.X. and P.H.; writing—original draft, C.X.; writing—review and editing, D.Z. and B.W.; supervision, J.Z.; H.Y. and Q.Z. All authors have read and agreed to the published version of the manuscript.

Funding: This research was supported by the Provincial School Joint Construction Project of Jilin Province, China (Grant no. SXGJXX2017-6); the Key Projects of Science and Technology Development Plan of Jilin Province, China (Grant no. 20170204015NY); and the National Key Research and Development Program of China (Grant no. 2016YFD070190103).

Conflicts of Interest: The authors declare no conflict of interest.

References

1. Xu, J.; Meng, J.H.; Quackenbush, L.J. Use of remote sensing to predict the optimal harvest date of corn. *Field Crop. Res.* **2019**, *236*, 1–13. [[CrossRef](#)]
2. Shao, Y.E.; Dai, J.T. Integrated Feature Selection of ARIMA with Computational Intelligence Approaches for Food Crop Price Prediction. *Complexity* **2018**, *2018*, 1910520. [[CrossRef](#)]
3. Ferraretto, L.F.; Shaver, R.D.; Luck, B.D. Recent advances and future technologies for whole-plant and fractionated corn silage harvesting. *J. Dairy Sci.* **2018**, *101*, 3937–3951. [[CrossRef](#)] [[PubMed](#)]
4. Han, W.; Li, G.; Yuan, M. Extraction Method of Maize Planting Information Based on UAV Remote Sensing Technology. *Trans. ASABE* **2017**, *48*, 139–147.
5. Zhang, L.; Chen, Z. Spatio-temporal Feature of Maize Production Efficiency in Main Producing Provinces of China. *Trans. ASABE* **2018**, *49*, 183–193.
6. Singh, V.; Stone, J.; Robert, J.P.; Vani, S.N. Industrial Biotechnology Shaping Corn Biorefineries of the Future. *Cereal Food World* **2019**, *64*. [[CrossRef](#)]
7. Eroglu, M.C.; Ogut, H.; Turker, U. Effects of some operational parameters in combine harvesters on grain loss and comparison between sensor and conventional measurement method. *Energy Educ. Sci. Technol.* **2011**, *28*, 497–504.
8. Liang, X.; Chen, Z.; Zhang, X.; Wei, L.; Li, W.; Che, Y. Design and Experiment of On-line Monitoring System for Feed Quantity of Combine Harvester. *Trans. ASABE* **2013**, *44*, 1–6.
9. Liang, Z.; Li, Y.; Xu, L. Grain Sieve Loss Fuzzy Control System in Rice Combine Harvesters. *Appl. Sci.* **2019**, *9*, 114. [[CrossRef](#)]
10. Maldaner, L.F.; de Paula Corrêdo, L.; Canata, T.F.; Molin, J.P. Predicting the sugarcane yield in real-time by harvester engine parameters and machine learning approaches. *Comput. Electron. Agric.* **2021**, *181*, 105945. [[CrossRef](#)]
11. Oksanen, T.; Linkolehto, R.; Seilonen, I. Adapting an industrial automation protocol to remote monitoring of mobile agricultural machinery: A combine harvester with IoT. *IFAC-Papers OnLine* **2016**, *49*, 127–131. [[CrossRef](#)]
12. Huang, Z.; Xue, J.; Ming, B.; Wang, K.; Xie, R.; Hou, P.; Li, S. Analysis of factors affecting the impurity rate of mechanically-harvested maize grain in China. *Int. J. Agric. Biol. Eng.* **2020**, *13*, 17–22. [[CrossRef](#)]
13. Baciewicz, F.A. Failure to Harvest Lymph Nodes. *Ann. Thorac. Surg.* **2019**, *107*, 1287. [[CrossRef](#)]
14. Jung, H.; Eshghi, A.T.; Lee, S. Structural Failure Detection Using Wireless Transmission Rate from Piezoelectric Energy Harvesters. *IEEE-ASME Trans. Mech.* **2020**, *1*, 1004. [[CrossRef](#)]
15. Wattanajitsiri, V.; Kanchana, R.; Triwanapong, S.; Kimapong, K. Identifying preventive maintenance guideline for a combine harvester with application of failure mode and effect analysis technique. In *MATEC Web of Conferences*; EDP Sciences: Les Ulis, France, 2020; Volume 134, pp. 187–194.
16. Monhollen, N.S.; Shinnors, K.J.; Friede, J.C.; Rocha, E.M.; Luck, B.D. In-field machine vision system for identifying corn kernel losses. *Comput. Electron. Agric.* **2020**, *174*, 105496. [[CrossRef](#)]
17. Chen, J.; Gu, Y.; Lian, Y.; Han, M. Online recognition method of impurities and broken paddy grains based on machine vision. *Trans. ASABE* **2018**, *34*, 187–194.
18. Jobbágy, J.; Dočkalík, M.; Krištof, K.; Burg, P. Mechanized grape harvester efficiency. *Appl. Sci.* **2021**, *11*, 4621. [[CrossRef](#)]
19. Zhang, Z.; Chi, R.; Du, Y.; Xie, B.; Deng, X.; Han, K. Investigation on CAN-bus-based Corn Harvester Intelligent Control System. *Trans. ASABE* **2018**, *49*, 275–281.
20. Mahirah, J.; Yamamoto, K.; Miyamoto, M.; Kondo, N.; Ogawa, Y.; Suzuki, T.; Habaragamuwaa, H.; Ahmad, U. Monitoring harvested paddy during combine harvesting using a machine vision-Double lighting system. *Eng. Agric. Environ. Food* **2017**, *10*, 140–149. [[CrossRef](#)]
21. Chen, M.; Ni, Y.; Jin, C.; Xu, J.; Yuan, W. High spectral inversion of wheat impurities rate for grain combine harvester. *Trans. ASABE* **2019**, *35*, 22–29.
22. Ran, J.; Wu, C. Application progress and development trend of sensor in grain combine harvester. *Jiangsu Agric. Sci.* **2019**, *47*, 23–29.
23. Giri, A.M.; Ali, S.F.; Arockiarajan, A. Dynamics of symmetric and asymmetric potential well-based piezoelectric harvesters: A comprehensive review. *J. Intell. Mater. Syst. Struct.* **2020**, *32*. [[CrossRef](#)]
24. Esmaeeli, R.; Aliniagerdroudbari, H.; Hashemi, S.R.; Alhadri, M.; Zakri, W.; Batur, C.; Farhad, S. Design, modeling, and analysis of a high performance piezoelectric energy harvester for intelligent tires. *Int. J. Energy Res.* **2019**, *43*, 5199–5212. [[CrossRef](#)]
25. Li, Y.; Tang, Z. *Design and Analysis of Grain Combine Harvester*; Machinery Industry Press: Beijing, China, 2014; p. 200.
26. Wang, J.; Shuai, S. *Automotive Engine Fundamentals*; Tsinghua University Press: Beijing, China, 2020; p. 127.
27. Ren, L. *Experimental Design and Optimization*; Science Press: Beijing, China, 2009; pp. 71–91.